arXiv:1007.4047v1 [cond-mat.str-el] 23 Jul 2010

Vortex Created by Skyrmion Spin Texture under Magnetic Field

Takao Morinari*
Yukawa Institute for Theoretical Physics, Kyoto University, Kyoto 606-8502, Japan
(Dated: July 26, 2010)

We show that a vortex current is created around a skyrmion spin texture under magnetic field due to a radial spin motive force in a two-dimensional metal with localized magnetic moments even in the absence of any superconductivity correlations. The effect is expected both for ferromagnetic and for antiferromagnetic systems. The Skyrmion-induced vortex mechanism provides a picture for large Nernst signals observed in the pseudogap phase of the high-T_c cuprates.

PACS numbers: 72.25.-b,72.15.Gd,74.72.-h

Skyrmions were originally proposed to describe baryons in terms of meson fields [1]. The central idea of constructing a topological object starting from an underlying field theory is widely used in many areas of physics [2]. In condensed matter physics the existence of skyrmions is suggested and confirmed in part in quantum Hall systems with filling fraction $\nu \simeq 1$ [3, 4], spinor Bose-Einstein condensate [5], itinerant ferromagnets [6], nematic liquid crystals [7], and high-temperature superconductors [8, 9]. From the topological nature of skyrmions the Berry phase effect [10] leads to an effective magnetic field, which has been studied intensively in various systems[11]. In this Letter I show that under magnetic field skyrmions create a vortex current due to spin motive force without relying on any superconductivity correlations. The skyrmion-induced vortex mechanism is applicable not only to ferromagnetic systems but also to antiferromagnetic systems.

In a two-dimensional isotropic ferromagnet, where the local magnetization direction vector is represented by $\mathbf{m} = (m_1, m_2, m_3)$, a skyrmion spin texture at the origin has the following form,

$$\mathbf{m}(\mathbf{r}) = \left(\frac{2\lambda x}{r^2+\lambda^2}, \frac{2\lambda y}{r^2+\lambda^2}, \frac{r^2-\lambda^2}{r^2+\lambda^2} \right), \tag{1}$$

where $r = \sqrt{x^2+y^2}$ and λ is the core size of the skyrmion. At infinity $\mathbf{m}$ approaches to the magnetization direction, which is taken as $\hat{e}_3$. (Hereafter $\hat{e}_j$ represents the unit vector in the j-axis.) This skyrmion spin texture is characterized by the topological charge,

$$Q = \frac{1}{4\pi} \int d^2\mathbf{r}\, \mathbf{m}(\mathbf{r}) \cdot \left[\partial_x \mathbf{m}(\mathbf{r}) \times \partial_y \mathbf{m}(\mathbf{r}) \right]. \tag{2}$$

If conduction electrons interact with $\mathbf{m}$ through an exchange coupling

$$\mathcal{H}_c = M J_c \int d^2\mathbf{r} \left[\psi^\dagger(\mathbf{r}) \boldsymbol{\sigma} \psi(\mathbf{r}) \right] \cdot \mathbf{m}(\mathbf{r}), \tag{3}$$

where M is the magnetization and the vector $\boldsymbol{\sigma}$ is $\boldsymbol{\sigma} = (\sigma_1, \sigma_2, \sigma_3)$ with σ_j the Pauli matrices, the Berry phase effect associated with the non-vanishing scalar chirality density $\mathbf{m}(\mathbf{r}) \cdot [\partial_x \mathbf{m}(\mathbf{r}) \times \partial_y \mathbf{m}(\mathbf{r})]$ produces an effective magnetic field effect for the conduction electrons. Anomalous Hall effect arising from such a Berry phase effect has been discussed in manganites [12], pyrochlores [13], and MnSi[14].

In this Letter, we study another Berry phase effect that emerges under magnetic field. The effect is associated with the spin motive force discussed in the context of spintronics [15] and experimentally observed recently [16]. If there is a domain wall, the spin motive force is induced along the domain wall under magnetic field. Here the same analysis is applied to skyrmion spin textures.

We start with a ferromagnetic metal,

$$\mathcal{H} = \int d^2\mathbf{r} \sum_{s=\uparrow,\downarrow} \psi_s^\dagger(\mathbf{r})\, \widehat{K}\left(-i\hbar\nabla\right) \psi_s(\mathbf{r}) + \mathcal{H}_c + \mathcal{H}_{\mathbf{m}}, \tag{4}$$

where $\hat{K}$ is the kinetic energy operator. The term $\mathcal{H}_{\mathbf{m}}$ describes the interaction for $\mathbf{m}$, and contains Dzyloshinsky-Moriya interactions. Here we assume that $\mathcal{H}_{\mathbf{m}}$ stabilizes a skyrmion texture for $\mathbf{m}$, and do not discuss explicit mechanisms for stabilizing a skrymion [17].

The coupling term $\mathcal{H}_c$ tends to align the conduction electron spin to $\mathbf{m}$. In order to include this correlation effect, we perform an SU(2) gauge transformation, $\psi(\mathbf{r}) \to U(\mathbf{r})\psi(\mathbf{r})$, where $U(\mathbf{r}) = \mathbf{n}(\mathbf{r}) \cdot \boldsymbol{\sigma}$ [18, 19] with

$$\mathbf{n}(\mathbf{r}) = \frac{(m_1(\mathbf{r}), m_2(\mathbf{r}), 1 + m_3(\mathbf{r}))}{\sqrt{2\left[1 + m_3(\mathbf{r})\right]}}. \tag{5}$$

The gauge potential associated with the SU(2) gauge transformation is given by $\mathbf{a} = -i\hbar U^\dagger \nabla U$ and $a_0 = i\hbar U^\dagger \partial_t U$. In terms of $\mathbf{n}$, we obtain

$$\mathbf{a} = \hbar \boldsymbol{\sigma} \cdot (\mathbf{n} \times \nabla \mathbf{n}), \tag{6}$$

$$a_0 = -\hbar \boldsymbol{\sigma} \cdot (\mathbf{n} \times \partial_t \mathbf{n}). \tag{7}$$

Note that $\partial_t \mathbf{n}$ is computed from the Heisenberg equation of motion. From these expressions we find the SU(2) gauge field,

$$\mathbf{e} = -2\hbar \boldsymbol{\sigma} \cdot (\partial_t \mathbf{n} \times \nabla \mathbf{n}), \tag{8}$$

$$\mathbf{b} = \hbar \varepsilon_{ijk} \sigma_i (\nabla n_j) \times (\nabla n_k), \tag{9}$$

where ε_{ijk} is the antisymmetric tensor.

Now we calculate the SU(2) gauge field created by a skrymion at the origin, Eq. (1). Introducing the cylindrical coordinate (r, ϕ, z), we obtain

$$\mathbf{b} = -\frac{2\hbar\lambda^2}{r\left(r^2+\lambda^2\right)^2}\begin{pmatrix} r & \lambda e^{-i\phi} \\ \lambda e^{i\phi} & -r \end{pmatrix}\hat{e}_z, \qquad (10)$$

and $\mathbf{e} = 0$. It is easy to see that $b_{zu} \equiv [b_z]_{\uparrow\uparrow}$ is equal to $\mathbf{m}\cdot\left(\partial_x\mathbf{m}\times\partial_y\mathbf{m}\right)/2$ [12]. The field b_{zu} behaves like a magnetic field for the conduction electrons. For $\lambda = 100\mathring{A}$, the average field strength is $\int_0^\lambda dr 2\pi r b_{zu}/(2\pi e\lambda^2) \simeq 3.3$ T. With decreasing λ, b_{zu} increases, and so b_{zu} can be very large. However, this effective field is not directly observable because it is not a real magnetic field.

Now we apply the magnetic field $\mathbf{B} = (0, 0, -B)$ to the system. From the Zeeman energy term the dynamics of $\mathbf{m}$ is given by

$$\frac{\partial}{\partial t}\mathbf{m} = \alpha\mathbf{B}\times\mathbf{m}, \qquad (11)$$

where $\alpha = gM\mu_B/\hbar$ with g the g-factor and μ_B the Bohr magneton. Using the solution of this equation of motion, we find

$$\mathbf{n}\left(\mathbf{r}, t\right) = \frac{\lambda\cos\Phi\left(t\right)\hat{e}_1 + \lambda\sin\Phi\left(t\right)\hat{e}_2 + r\hat{e}_3}{\sqrt{r^2+\lambda^2}}, \qquad (12)$$

with $\Phi\left(t\right) = \phi - \alpha B t + \phi_0$. ($\phi_0$ is a constant.) The field $\mathbf{b}$ is given by Eq. (10) with ϕ being replaced by $\Phi(t)$. Now the field $\mathbf{e}$ is nonzero and given by

$$\mathbf{e} = \frac{2\alpha B\hbar\lambda^2}{\left(r^2+\lambda^2\right)^2}\begin{pmatrix} r & \lambda e^{-i\Phi(t)} \\ \lambda e^{i\Phi(t)} & -r \end{pmatrix}\hat{e}_r \qquad (13)$$

Note that the effective field $\mathbf{e}$ is created in the radial direction [20]. This is understood as follows. If one sees the skyrmion spin texture along a straight line crossing the origin in the x-y plane, the spin configuration looks like a domain wall. From the analysis of the domain wall we know that the spin motive force is created along it [15]. The same is true in each direction. Thus, the spin motive force $\mathbf{e}$ is created in the radial direction for skyrmion spin textures.

Since e_{zu} is non-zero and there is the external magnetic field and b_{zu}, a drift of conduction electrons is induced. The drift is circular around the skyrmion because e_{zu} is in the radial direction. Thus, the drift motion leads to the vortex current. The drift velocity is

$$v_\phi = \frac{2\alpha B\lambda^2 r}{2\lambda^2 + \left(eB/\hbar\right)\left(r^2+\lambda^2\right)^2}. \qquad (14)$$

Figure 1 shows this drift velocity as a function of r/λ. For $r/\lambda < 1$, b_{zu} plays a major role for the drift. While for $r/\lambda > 1$, B plays a major role. For $B > 0$ the external magnetic field is parallel to b_{zu}. If we consider an anti-skyrmion, the drift velocity changes its direction at $r = \sqrt{\lambda\left(\sqrt{2}\ell_B - \lambda\right)}$ with $\ell_B = \sqrt{eB/\hbar}$ the magnetic length. We do not consider this case in the following analysis because such a current distribution is energetically unfavorable, though it is not forbidden.

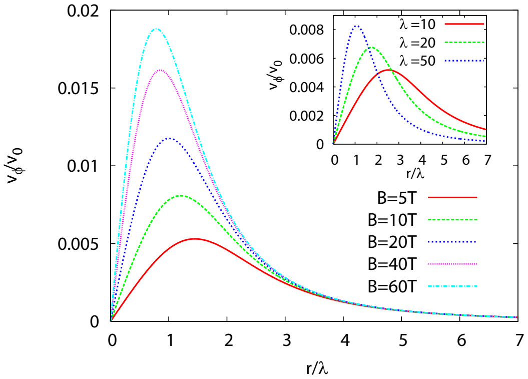

FIG. 1. (color online) The drift velocity as a function of r/λ for different magnetic fields at $\lambda = 40\mathring{A}$ with $v_0 = gMc$ with c the speed of light. The inset shows the drift velocity versus r/λ for different λ (in units of $\mathring{A}$) at $B = 10$ T.

The circular drift velocity (14) leads to a vortex current. The magnetic field B_v created by this vortex current is computed as in that for vortex current in a layered superconductor [21]:

$$B_v = \int_0^\infty dq q J_0\left(q\rho\right) A_0\left(q\right)\exp\left(-q\left|z\right|\right), \qquad (15)$$

$$A_0\left(q\right) = -\frac{2\pi}{c}\int_0^\infty d\rho\rho J_1\left(q\rho\right)\left(\mathbf{j}_{2\mathrm{d}}\right)_\phi, \qquad (16)$$

with $J_n(x)$ the Bessel function and the two-dimensional current density is $\left(\mathbf{j}_{2\mathrm{d}}\right)_\phi = en_{2\mathrm{d}}v_\phi$. Here $n_{2\mathrm{d}}$ is the two-dimensional conduction electron density. This magnetic field B_v is shown in Fig. 2. The field is measured in units of tesla and is normalized by a dimensionless parameter $B_0 = gMn_{2\mathrm{d}}\lambda^2$. Note that usually vortex currents are induced if there is a superconductivity correlation. However, the skyrmion-induced vortex current does not require any superconductivity correlations.

The same formula can be applied to the antiferromagnetic case as well. Let us consider a square lattice and introduce A and B sublattice. For this case we take $\mathbf{m}(\mathbf{r})$ as the local staggered magnetization direction vector. The conduction electron spin residing at $\mathbf{R}_j$ is aligned to $\mathbf{m}(\mathbf{R}_j)$ by the unitary transformation matrix $U(\mathbf{R}_j)$. Carrying out this transformation, we obtain the same Hamiltonian except for the exchange interaction term. The sign of the exchange interaction term is different for A and B sublattice. In the strong coupling limit, the conduction electron spin at B sublattice is anti-parallel

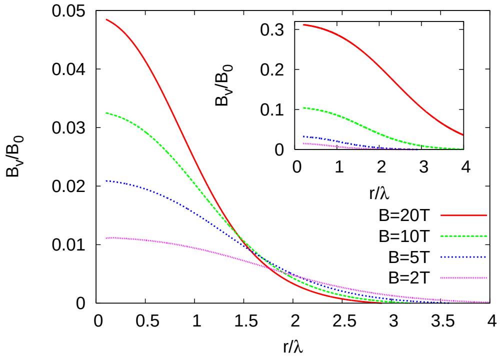

FIG. 2. (color online) The magnetic field B_v created by the vortex current for different magnetic field at $z = 0$ with $\lambda = 40\AA$. The inset shows B_v for $\lambda = 10, 20, 40, 60$ (in units of $\AA$) from top to bottom.

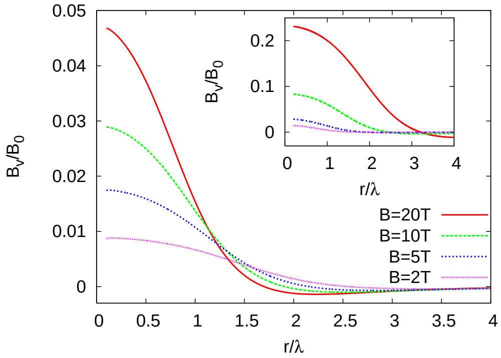

FIG. 3. (color online) The magnetic field B_v as a function of r/λ for the antiferromagnetic case. The value of B_v is computed for different magnetic field at $z = 0$ with $\lambda = 40\AA$. The inset shows B_v for $\lambda = 10, 20, 40, 60$ (in units of $\AA$) from top to bottom.

to that at A sublattice. The relevant components of the SU(2) fields are

$$[\mathbf{e}]_{\uparrow\downarrow} = ([\mathbf{e}]_{\downarrow\uparrow})^* = \frac{2\alpha B\hbar\lambda^3}{(r^2+\lambda^2)^2} e^{-i\Phi}\hat{e}_r, \tag{17}$$

$$[\mathbf{b}]_{\uparrow\downarrow} = ([\mathbf{b}]_{\downarrow\uparrow})^* = -\frac{2\hbar\lambda^3}{r\,(r^2+\lambda^2)^2} e^{-i\Phi}\hat{e}_z. \tag{18}$$

Note that the SU(2) gauge fields acting on the conduction electrons are not staggered, in spite of the fact that the magnetization direction vector is staggered. Denoting $\mathbf{e} = \sum_j \mathbf{e}_j\sigma_j$ and $\mathbf{b} = \sum_j \mathbf{b}_j\sigma_j$, we find the gauge field components $\mathbf{e}_j$ and $\mathbf{b}_j$. For a bond vector connecting from B sublattice to A sublattice, these components take opposite sign compared to the case of a bond vector connecting from A sublattice to B sublattice. A crucial point is that this sign change cancel completely in the drift created by $\mathbf{e}$ and $\mathbf{b}$. The situation is clearer if we carry out an additional Unitary transformation $V = \exp(i\Phi\sigma_z/2)$ that makes $\mathbf{e}_{\uparrow\downarrow} = \mathbf{e}_{\downarrow\uparrow}$ and $\mathbf{b}_{\uparrow\downarrow} = \mathbf{b}_{\downarrow\uparrow}$ and removes the sign change. The drift velocity calculation is similar to the ferromagnetic case, and we obtain

$$v_\phi = \frac{2\alpha B\lambda^3 r}{2\lambda^3 + (eB/\hbar)\,r\,(r^2+\lambda^2)^2}. \tag{19}$$

The difference arises from the relevant component of the gauge fields as stated above. Figure 3 shows the magnetic field created by the drift calculated by Eqs. (15) and (16) using Eq. (19). Although r dependence of the effective fields are different between the antiferromagnetic case and the ferromagnetic case, the results are similar. For $r < \lambda$, the effective field $\mathbf{b}$ plays a major role for the drift. In this regime, the drift velocity has the same form as that for the ferromagnetic case. This is the reason why we obtained similar results for both cases for $r < \lambda$. Meanwhile for $r > \lambda$ the effective electric field is suppressed by the factor λ/r. Thus, B_v decreases rapidly compared to the ferromagnetic case.

In order to stabilize the vortex current, we need to keep the radial effective electric field $\mathbf{e}$. However, in general a radial electric field is screened by conduction electrons. Therefore, to stabilize the vortex current the Thomas-Fermi length, which is proportional to $1/n_{2\mathrm{d}}$, should be larger than λ, otherwise the effective electric field is screened by the conduction electrons.

Now it is natural to ask a question: What is the difference between the vortex current arising from the skyrmion spin texture and a conventional vortex arising from a superconductivity correlation? As long as the external magnetic field is kept, the skyrmion-induced vortex current continues to flow even in the presence of dissipations. However, the current decays rapidly when one turns off the magnetic field. This makes the crucial difference compared to conventional vortices in a superconductor. In addition, the flux quantization occurs only for a mesoscopic sample.

In the formulation above we have assumed that there is magnetic long-range order. But this assumption is not necessary. Suppose the system does not have magnetic long-range order and let ξ be the magnetic correlation length. For $\xi \gg \lambda$, we may apply the formula above to the system as well. If ξ is comparable to λ, the field $\mathbf{b}$ and $\mathbf{e}$ are multiplied by the factor $\exp(-2r/\xi)$, and M should be replaced by the average of spins over the domain. The amplitude of the fields would decrease by these factors but one may still expect a vortex formation.

So far we have assumed that skyrmions are static. However, it is possible to consider a moving skyrmion [22] and compute a vortex current around it. For a moving skyrmion, the antiferromagnetic case is much better than the ferromagnetic case. If one adopts the non-linear

σ model for the description of the skyrmion spin texture, the skyrmion is a soliton solution of the non-linear σ model. However, for the ferromagnetic case the skyrmion spin texture is stable only for the static case. Because of the quadratic dispersion of spin waves, the chiral nature of the skyrmion spin texture is lost upon skyrmion propagation. By contrast, for the antiferromagnetic case a moving skyrmion spin texture solution is constructed by a Lorentz boost. This is possible because the non-linear σ model has a relativistic form. Of course there are deviations from the relativistic dynamics in the real system, and those deviations would lead to a finite life time even in the antiferromagnetic case.

In order to observe the vortex currents predicted above candidate systems are $\mathrm{Fe}_{1-x}\mathrm{Co}_x\mathrm{Si}$, where real-space observation of a two-dimensional skyrmion crystal was reported [23], and MnSi, where magnetoresistance measurements suggest the presence of skyrmions [14]. Another interesting application of the theory is that for cuprate high-temperature superconductors. In recent experiments large Nernst effects were observed[24] above the superconductivity transition temperature T_c. For the single band system, which is believed to be the case for the high-T_c, the Nernst effect is absent because of Sondheimer cancellation[24]. One scenario for the large Nernst effect above T_c is to assume the presence of preformed Cooper pairs. Assuming a skyrmion texture carried by a doped hole provides an alternative scenario. To make clear whether the skyrmion spin texture is formed in the high-T_c cuprates or not, the best way would be to investigate Li-doped underdoped samples. Establishing a skyrmion spin texture by observing the vortex current around a doped hole bound to a Li ion provides a crucial step to uncover the mechanism of cuprate high-temperature superconductivity [25].

To conclude, we have discussed a mechanism of vortex current formation under magnetic field based on the skyrmion spin texture without relying on any superconductivity correlations. The vortex current is created for antiferromagnetic systems as well as ferromagnetic systems. The presence of the vortex can be verified by observing the magnetic field created by the vortex current. Searching for a skyrmion-induced vortex current in underdoped cuprates would be a key step to justify the relevance of the skyrmion spin texture in high-T_c.

I would like to thank M. Sigrist for helpful discussions. This work was supported by the Global COE Program "The Next Generation of Physics, Spun from Universality and Emergence," and Yukawa International Program for Quark-Hadron Sciences at YITP.

---

* morinari@yukawa.kyoto-u.ac.jp

[1] T. Skyrme, Proceedings of the Royal Society of London. Series A, Mathematical and Physical Sciences **260**, 127 (1961); Nucl. Phys **31**, 556 (1962).

[2] *The Multifaceted Skyrmion*, edited by G. E. Brown and M. Rho (World Scientific, 2010).

[3] S. L. Sondhi, A. Karlhede, S. A. Kivelson, and E. H. Rezayi, Phys. Rev. B **47**, 16419 (1993).

[4] S. E. Barrett, G. Dabbagh, L. N. Pfeiffer, K. W. West, and R. Tycko, Phys. Rev. Lett. **74**, 5112 (1995).

[5] L. S. Leslie, A. Hansen, K. C. Wright, B. M. Deutsch, and N. P. Bigelow, Phys. Rev. Lett. **103**, 250401 (2009).

[6] U. Rößler, A. Bogdanov, and C. Pfleiderer, Nature **442**, 797 (2006); B. Binz, A. Vishwanath, and V. Aji, Phys. Rev. Lett. **96**, 207202 (2006); S. Tewari, D. Belitz, and T. R. Kirkpatrick, **96**, 047207 (2006).

[7] A. N. Bogdanov, U. K. Rößler, and A. A. Shestakov, Phys. Rev. E **67**, 016602 (2003).

[8] B. I. Shraiman and E. D. Siggia, Phys. Rev. B **42**, 2485 (1990); R. J. Gooding, Phys. Rev. Lett. **66**, 2266 (1991); S. Haas, F.-C. Zhang, F. Mila, and T. M. Rice, **77**, 3021 (1996); T. Morinari, in *The Multifaceted Skrymion* (World Scientific, 2010); A. R. Pereira, E. Ercolessi, and A. S. T. Pires, J. Phys. Condens. Matter **19**, 156203 (2007).

[9] I. Raicevic, D. Popovic, C. Panagopoulos, L. Benfatto, M. Neto, E. Choi, and T. Sasagawa, Arxiv preprint arXiv:1006.1891(2010).

[10] M. V. Berry, Proc. R. Soc. A **392**, 45 (1984).

[11] See, for a review, N. Nagaosa, J. Sinova, S. Onoda, A. H. MacDonald, and N. P. Ong, Rev. Mod. Phys. **82**, 1539 (2010).

[12] J. Ye, Y. B. Kim, A. J. Millis, B. I. Shraiman, P. Majumdar, and Z. Tešanović, Phys. Rev. Lett. **83**, 3737 (1999); P. Matl, N. P. Ong, Y. F. Yan, Y. Q. Li, D. Studebaker, T. Baum, and G. Doubinina, Phys. Rev. B **57**, 10248 (1998).

[13] T. Taguchi, Y. Oohara, H. Yoshizawa, N. Nagaosa, and Y. Tokura, Science **291**, 2573 (2001).

[14] M. Lee, W. Kang, Y. Onose, Y. Tokura, and N. P. Ong, Phys. Rev. Lett. **102**, 186601 (2009); A. Neubauer, C. Pfleiderer, B. Binz, A. Rosch, R. Ritz, P. G. Niklowitz, and P. Böni, **102**, 186602 (2009); C. Timm, Physics **2**, 35 (2009).

[15] S. E. Barnes and S. Maekawa, Phys. Rev. Lett. **98**, 246601 (2007).

[16] P. Hai, S. Ohya, M. Tanaka, S. Barnes, and S. Maekawa, Nature **458**, 489 (2009); S. A. Yang, G. S. D. Beach, C. Knutson, D. Xiao, Q. Niu, M. Tsoi, and J. L. Erskine, Phys. Rev. Lett. **102**, 067201 (2009).

[17] See Ref. [6] for discussions about $\mathcal{H}_{\mathbf{m}}$.

[18] V. Korenman, J. L. Murray, and R. E. Prange, Phys. Rev. B **16**, 4032 (1977); G. Volovik, J. Phys. C **20**, L83 (1987).

[19] Y. Tserkovnyak and M. Mecklenburg, Phys. Rev. B **77**, 134407 (2008).

[20] A similar calculation was presented in C. H. Wong and Y. Tserkovnyak, Phys. Rev. B **80**, 184411 (2009).

[21] J. R. Clem, Phys. Rev. B **43**, 7837 (1991).

[22] A numerical simulation of a moving spin texture based on the Landau-Lifshitz-Gilbert equation was carried out in J.-i. Ohe, S. E. Barnes, H.-W. Lee, and S. Maekawa, Appl. Phys. Lett. **95**, 123110 (2009) under inplane magnetic field

[23] X. Yu, Y. Onose, N. Kanazawa, J. Park, J. Han, Y. Matsui, N. Nagaosa, and Y. Tokura, Nature **465**, 901 (2010).

[24] Y. Wang, L. Li, and N. P. Ong, Phys. Rev. B **73**, 024510 (2006).

[25] Recent magnetization and magnetoresistance measurements[9] suggested the presence of skyrmions in insulating antiferromagnet $La_2Cu_{0.97}Li_{0.03}O_4$.